

Significant enhancement of photovoltage in artificially designed perovskite oxide structures

Wen-jia Zhou, Kui-juan Jin, Hai-zhong Guo, Xu He, Meng He, Xiu-lai Xu, Hui-bin Lu, and Guo-zhen Yang

Citation: *Applied Physics Letters* **106**, 131109 (2015); doi: 10.1063/1.4916993

View online: <http://dx.doi.org/10.1063/1.4916993>

View Table of Contents: <http://scitation.aip.org/content/aip/journal/apl/106/13?ver=pdfcov>

Published by the **AIP Publishing**

Articles you may be interested in

[Photovoltaic effect in an indium-tin-oxide/ZnO/BiFeO₃/Pt heterostructure](#)

Appl. Phys. Lett. **105**, 162903 (2014); 10.1063/1.4899146

[Optimization on photoelectric detection based on stacked La_{0.9}Sr_{0.1}MnO_{3-δ}/LaAlO_{3-δ} multijunctions](#)

J. Appl. Phys. **110**, 033103 (2011); 10.1063/1.3621143

[Charge separation and recombination in radial ZnO / In₂S₃ / CuSCN heterojunction structures](#)

J. Appl. Phys. **108**, 044915 (2010); 10.1063/1.3466776

[A theoretical study on the dynamic process of the lateral photovoltage in perovskite oxide heterostructures](#)

Appl. Phys. Lett. **96**, 062116 (2010); 10.1063/1.3313943

[Photovoltaic effect in micrometer-thick perovskite-type oxide multilayers on Si substrates](#)

Appl. Phys. Lett. **93**, 171911 (2008); 10.1063/1.3010373

Frustrated by old technology? Is your AFM dead and can't be repaired? Sick of bad customer support?

It is time to upgrade your AFM
Minimum \$20,000 trade-in discount
for purchases before August 31st

**Asylum Research is today's
technology leader in AFM**

dropmyoldAFM@oxinst.com

**OXFORD
INSTRUMENTS**
The Business of Science®

Significant enhancement of photovoltage in artificially designed perovskite oxide structures

Wen-jia Zhou,¹ Kui-juan Jin,^{1,2,a)} Hai-zhong Guo,¹ Xu He,¹ Meng He,¹ Xiu-lai Xu,¹ Hui-bin Lu,¹ and Guo-zhen Yang^{1,2}

¹Beijing National Laboratory for Condensed Matter Physics, Institute of Physics, Chinese Academy of Sciences, Beijing 100190, People's Republic of China

²Collaborative Innovation Center of Quantum Matter, Beijing 100190, China

(Received 26 December 2014; accepted 26 March 2015; published online 2 April 2015)

La_{0.9}Sr_{0.1}MnO₃/insulator/SrNb_{0.007}Ti_{0.993}O₃ multilayer and La_{0.9}Sr_{0.1}MnO₃/SrNb_{0.007}Ti_{0.993}O₃/In₂O₃:SnO₂(ITO)/La_{0.9}Sr_{0.1}MnO₃/SrNb_{0.007}Ti_{0.993}O₃ multilayer structures were designed to enhance the photovoltage. The photovoltages of these two structures under an illumination of 308 nm laser are 410 and 600 mV, respectively. The latter is 20 times larger than that (30 mV) observed in La_{0.9}Sr_{0.1}MnO₃/SrNb_{0.007}Ti_{0.993}O₃ single junction. The origin of such significant enhancement of photovoltage is discussed in this letter. These results suggest that the photoelectric property of perovskite oxides could be much improved by artificial structure designing. The enhanced photovoltaic effects have potential applications in the ultraviolet photodetection and solar cells. © 2015 AIP Publishing LLC. [<http://dx.doi.org/10.1063/1.4916993>]

Perovskite oxide heterostructures, which can exhibit interesting novel properties such as conducting two dimensional electron gas at the interface between the insulating oxide materials LaAlO₃ and SrTiO₃^{1–3} and positive colossal magnetoresistance,^{4,5} have attracted significant attentions in recent years. The interest comes also from the perspective of designing and tuning specific properties to achieve desired functionalities.⁶ As one of the important properties, the photoelectric effect of perovskite oxide heterostructures and correlative devices has been investigated by many groups due to their potential applications in UV detection and energy area.^{7–9} Assmann *et al.* proposed high efficient solar cells with LaVO₃/SrTiO₃ heterostructures,¹⁰ and ultrafast photoelectric effect was also discovered in La_{0.9}Sr_{0.1}MnO₃ (LSMO) heterostructures.^{11–15} Moreover, a large lateral photovoltage induced by Dember effect was observed in LSMO/Si heterostructures.¹⁶ Among all the investigations, one issue needs to be solved is to improve the photovoltage of the perovskite oxide heterostructures. For this purpose, side illumination and many other methods were proposed.^{17–19} Previously, we have reported an ultimate value of photovoltage in the heterostructures with a film thickness consistent with the calculated thickness of the depletion layer in LSMO films for heterostructures of LSMO/SrNb_{0.008}Ti_{0.992}O₃ and LSMO/Si.^{7,20} In this work, we designed two kinds of multilayer structures, and obtained as much as 20 times larger photovoltage than that in the single heterostructures. The mechanism behind this dramatically enhancement is discussed.

The following two kinds of multilayer structures are proposed: one is LSMO/insulator (SrTiO₃ or BaTiO₃)/SrNb_{0.007}Ti_{0.993}O₃ (SNT0) multilayer structure and the other is LSMO/SNT0/In₂O₃:SnO₂(ITO)/LSMO/SNT0 multilayer structure, for the purpose of further enhancing the

photovoltage by artificial structure design. The structures of LSMO (20 nm)/insulator (10 nm)/SNT0 (substrate) and LSMO (20 nm)/SNT0 (10 nm)/ITO (10 nm)/LSMO (20 nm)/SNT0 (substrate) were deposited by a computer-controlled laser molecular beam epitaxy equipped with an *in situ* reflection high-energy electron diffraction (RHEED) system (PASCAL). The growth was performed with a base pressure 1×10^{-6} Pa. XeCl excimer laser (308 nm, 20 ns, and 2.2 J cm^{-2}) was used during the fabrication. When growing the ITO interlayer, laser frequency was chosen at 6 Hz, while 2 Hz was chosen when fabricating all other layers. The films were grown at 950 °C and an oxygen pressure of 10 Pa. As a reference, a single LSMO/SNT0 junction was fabricated in the same situation. The thicknesses of LSMO thin films in all kinds of heterostructures were monitored by the RHEED system. After the deposition, the samples were characterized by high-resolution Synchrotron X-ray diffractometry (SXRD) using the BL14B1 beam line of Shanghai Synchrotron Radiation Facility (SSRF) and atomic force microscopy (AFM). As for the photoelectrical measurements, platinum electrode with a diameter of 400 μm was deposited on the *p*-type LSMO films and Indium was used as the electrode of the *n*-type SNT0 to form ohmic contacts. The photoelectric properties were investigated by using light sources with various wavelengths from 300 to 600 nm. The photovoltaic signals were recorded by a 500 MHz sampling oscilloscope with an input impedance of 1 MΩ. The electrodes were always kept in the dark during the experiments to avoid possible effects. The current-voltage curves were measured using a Keithly 2400 electrometer.

Figure 1(a) displays a typical RHEED intensity oscillation curve during the growth of the first LSMO layer on the SNT0 substrate. The intensity oscillation infers a two-dimensional lay-by-layer growth mode. Though the oscillation disappears when the roughness increases, the RHEED image of as-grown multilayer taken at the end of all the deposition is still sharp, as shown in the inset of Fig. 1(a), which

^{a)}Author to whom correspondence should be addressed. E-mail: kjjin@iphy.ac.cn

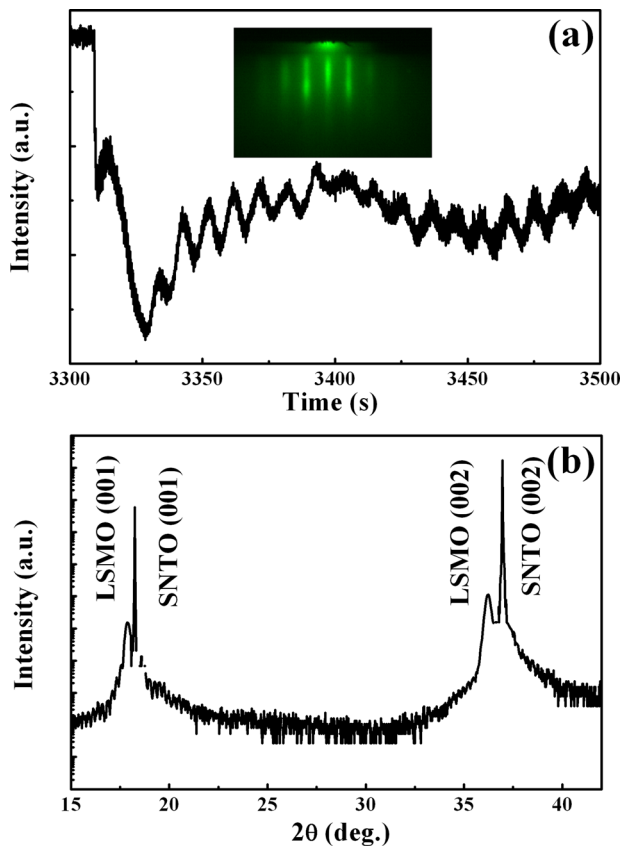


FIG. 1. (a) RHEED intensity oscillation during the growth of the first LSMO layer on the SNTNO substrate. (b) SXRD pattern of the LSMO/SNTNO/ITO/SNTNO/LSMO multilayer. The inset in (a) is a RHEED pattern of the structure after depositing all the layers.

confirms a good crystallinity and a smooth surface. AFM topography also supports this conclusion (not shown here). Figure 1(b) exhibits the SXRD pattern of the LSMO/SNTNO/ITO/LSMO/SNTNO multilayer structure. As shown in

Fig. 1(b), the θ - 2θ scan has no indication of the presence of additional phases other than (001) oriented layers. As for the LSMO/insulator/SNTNO multilayer, we did the same investigation and obtained the similar conclusion.

As we reported earlier,²⁰ an ultimate value of photovoltage in the heterostructures with the film thickness is consistent with the calculated thickness of the depletion layer in LSMO films for heterostructures of LSMO/SNTNO. Therefore, the photovoltage of a heterojunction is proposed to be related to its thickness of the depletion layer. Thus, after inserting the insulator layer, the width of the depletion layer should be changed and the properties of the junction can be tuned. With such a motivation, we designed two LSMO/insulator/SNTNO multilayer structures and checked their properties. Figures 2(a) and 2(b) exhibit the I - V curves of the LSMO/insulator/SNTNO multilayer structure in dark environment and under light (375 nm, 5.1 mW/mm²), respectively. Both LSMO/BTO/SNTNO and LSMO/STO/SNTNO have a smaller current than that of LSMO/SNTNO under the same voltage. The reason can be attributed to the increase of the width of the depletion layer due to inserting an insulator.²¹ Under the illumination of light, the I - V curves of LSMO/BTO/SNTNO and LSMO/STO/SNTNO both have a larger offset than that of the LSMO/SNTNO. As we all know, the offset indicates the generation of an open circuit voltage. Figures 2(c) and 2(d) show the photovoltages of the LSMO/insulator/SNTNO structures and the reference LSMO/SNTNO structure under different light sources. Under 308-nm-pulse laser (20 ns, 0.5 mJ/mm²), LSMO/BTO/SNTNO and LSMO/STO/SNTNO multilayers have a photovoltage of 410 and 290 mV, respectively, while the reference single junction of LSMO/SNTNO only has a photovoltage of 30 mV. For the 375-nm continuous-wave laser (5.1 mW/mm²), the photovoltages of LSMO/BTO/SNTNO, LSMO/STO/SNTNO, and LSMO/SNTNO are 140, 49, and 5 mV, respectively. As

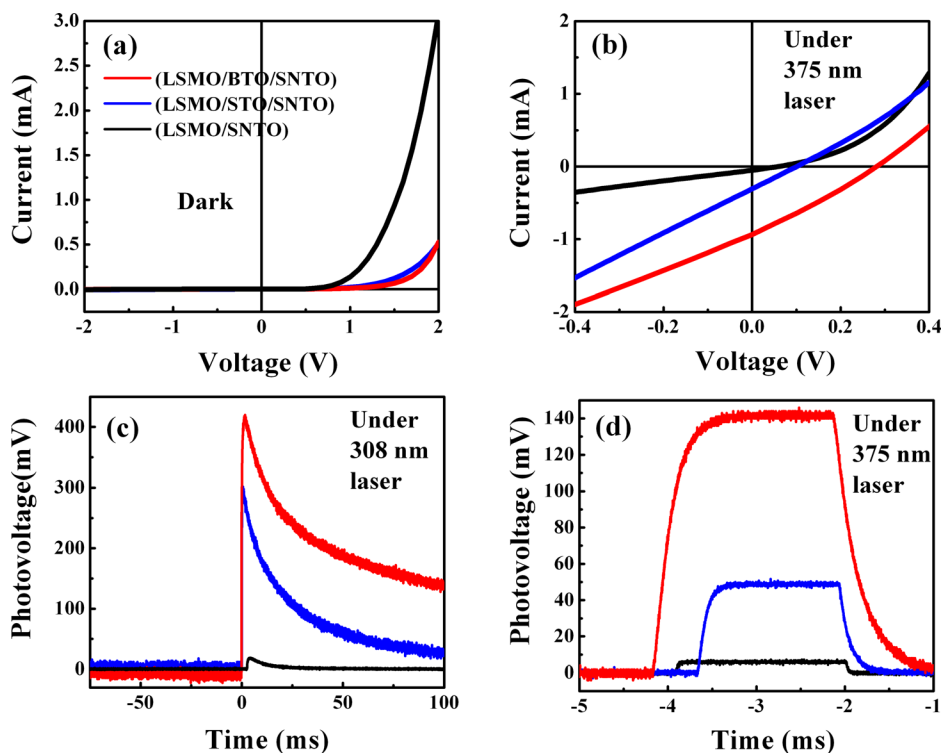


FIG. 2. (a) I - V curve of the LSMO/insulator/SNTNO multilayer and its reference single junction in the dark. (b) I - V curve of the LSMO/insulator/SNTNO multilayer and its reference single junction under 375 nm laser (5.1 mW/mm²). (c) Photovoltage of the LSMO/insulator/SNTNO multilayer and its reference single junction under the illumination of 308 nm laser (20 ns, 0.5 mJ/mm²). (d) Photovoltage of the LSMO/insulator/SNTNO multilayer and its reference single junction under the illumination of 375 nm laser (5.1 mW/mm²).

expected, the photovoltage of the heterostructure with inserting layer is enhanced comparing to the one without the inserting layer.

In order to further improve the photovoltage, we designed a multilayer with LSMO/SNTO/ITO/LSMO/SNTO structure. Figure 3(a) shows the I - V curves of the multilayer structure and the reference LSMO/SNTO in the dark environment. Both the samples exhibit good nonlinear and rectifying I - V characteristics. In darkness, the I - V curves should pass through the origin of coordinate. When the samples are under illumination, photo-generated carriers are generated and there are photocurrents and photovoltages in the heterostructures, which are superimposed on the values of the I - V curves in the darkness; therefore, the I - V curves under illumination have offsets comparing with that in darkness and these offsets are related to the photovoltage. Thus, we can characterize the photovoltage with the observed offsets of the I - V curves. Figure 3(b) shows the I - V curves of the multilayer structure under an illumination of UV light (375 nm laser, 5.1 mW/mm^2). It can be seen that the offset of the multilayer structure is bigger than the single junction. Therefore, we can predict that the multilayer structure can generate a larger photovoltage than the single junction.

Then the photovoltage under the illumination of 308 nm laser (20 ns, 0.5 mJ/mm^2) was studied. Because the photon energy of laser pulse (4.0 eV) is larger than the band gap of LSMO ($\sim 1.0 \text{ eV}$) and SNTO ($\sim 3.2 \text{ eV}$),²² when the laser illuminates the sample surface, the photons will be absorbed. Considering that the transmissivity of 10-nm-thick ITO is about 70%²³ and the photoabsorption coefficient α of LSMO and SNTO are $1.5 \times 10^5 \text{ cm}^{-1}$ and $1.2 \times 10^5 \text{ cm}^{-1}$,

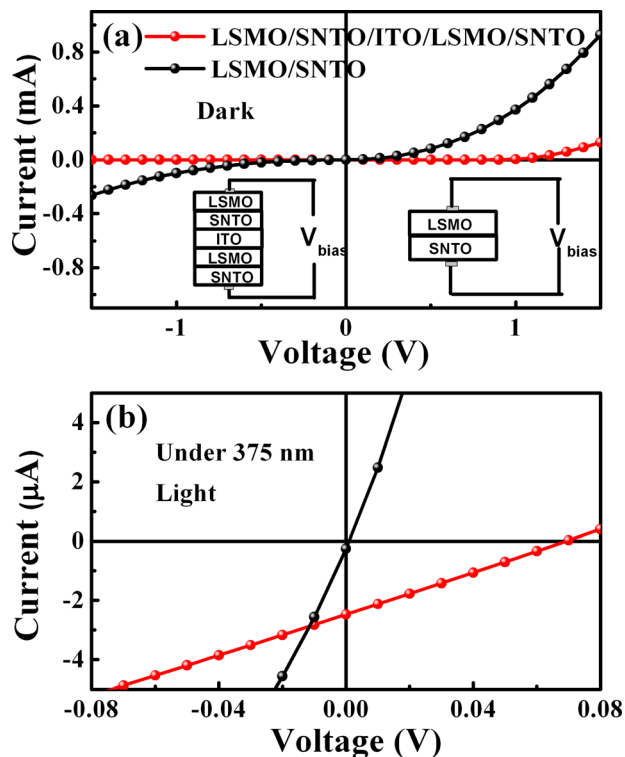


FIG. 3. (a) I - V curve of the LSMO/SNTO/ITO/SNTO/LSMO multilayer and its reference single junction in the dark. (b) I - V curve of the LSMO/SNTO/ITO/SNTO/LSMO multilayer and its reference single junction under 375 nm laser (5.1 mW/mm^2). The insets in (a) are the schematics of measurement.

respectively,²⁴ according to the formula $I = I_0 \exp(-\alpha x)$, where I and I_0 stand for the light intensity before and after illumination while x is the material thickness. As all films in the multilayer structure are much thinner than their absorption lengths, we believe that all the layers of the multilayer structure can absorb the photons, and are involved in the generation of the photovoltage in the system. Figure 4 shows the photovoltage of the LSMO/SNTO/ITO/LSMO/SNTO multilayer and the reference LSMO/SNTO single junction at ambient temperature, respectively. At the same condition, it is shown that the multilayer structure has a photovoltage of about 600 mV, while the reference single junction only about 30 mV. That is to say, the photovoltage of the multilayer structure is greatly enhanced comparing to the single one.

We also investigated the photovoltage of the multilayer structure without ITO interlayer (LSMO/SNTO/LSMO/SNTO structure), no photovoltage signal was measured. This phenomenon clarified that the ITO interlayer plays an important role in enhancing the photovoltaic of the multilayer. The wavelength we used is 308 nm and the bandgap of ITO is around 4.0 eV,²⁵ therefore photogenerated carriers can be generated in ITO layer and may contributed to the photovoltage. For LSMO/SNTO/LSMO/SNTO structure, there is no ITO layer and no photogenerated carriers in ITO interlayer. On the other hand, without ITO interlayer, the LSMO layer in the lower junction and the SNTO layer in the upper junction are directly contacted and will form an inverse junction, which will also prevent the generation of the photovoltage. In order to further understand the role of the ITO interlayer, samples with ITO interlayer of different thickness were fabricated in the same condition. Their photovoltaic properties were shown in the inset of Fig. 4. It can be seen that with the increase of the thickness of ITO, the photovoltage of the multilayer also increases.

The wavelength responsivity was also investigated by using different wavelengths of light source. Figures 5(a)–5(c) display the photovoltaic signals under a 600-nm laser, 375-nm laser, and 300-nm laser, respectively. The energy densities are all 5.1 mW/mm^2 . Under all these lasers, it is obvious that the photovoltages are greatly enhanced comparing to the reference single junction LSMO/SNTO. Under the 300-nm

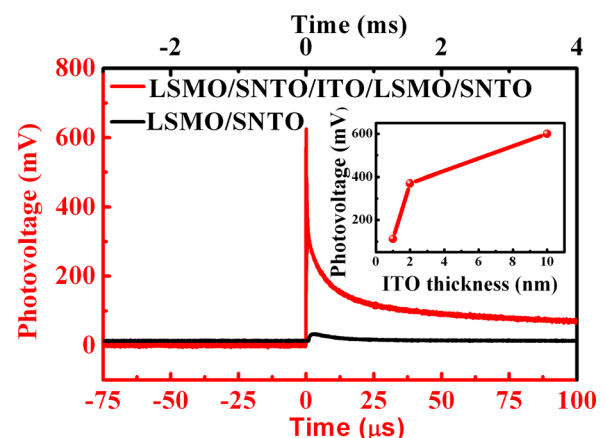


FIG. 4. Photovoltage of the LSMO/SNTO/ITO/LSMO/SNTO multilayer and its reference single junction under the illumination of 308 nm laser (20 ns, 0.5 mJ/mm^2). The inset is the dependence of the photovoltage of multilayer on the thickness of the ITO layer.

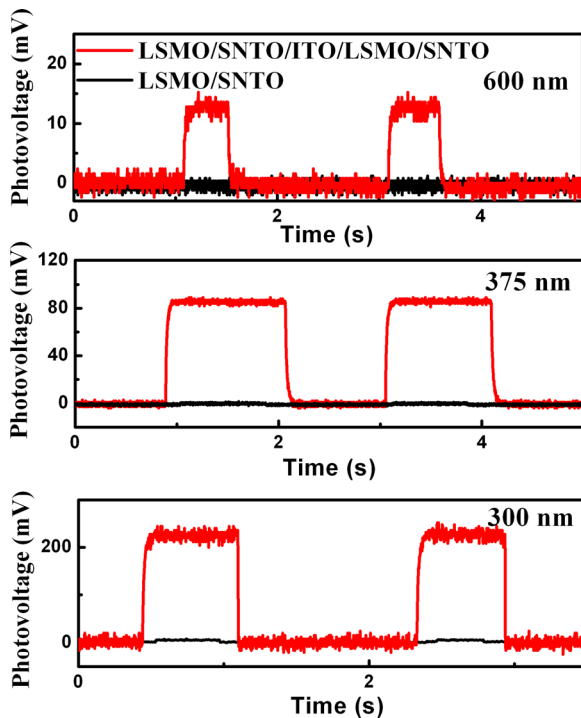


FIG. 5. Photovoltage of the LSMO/SNTO/ITO/LSMO/SNTO multilayer and its reference single junction under the illumination of (a) 600 nm (b) 375 nm, and (c) 300 nm laser. The energy densities for three measurements are 5.1 mW/mm^2 .

laser, the photovoltage of the multilayer is 200 mV and the reference one is 10 mV. Under the 375 nm laser, the photovoltages are 80 and 5 mV, respectively. However, under the 600-nm laser, the multilayer shows a photovoltage of 15 mV, while the reference junction shows no photovoltaic signal. The band gaps of LSMO and SNTO are 1.0 and 3.2 eV,²² respectively. Because the photon energy of 600 nm is 2.07 eV, which cannot be absorbed by the SNTO layer, only the LSMO layer attributes to the photovoltaic, while for the 300-nm laser and 375-nm laser, both the LSMO and SNTO layers can absorb the light and attributes to the photovoltage. This is the reason why the photovoltage under 600 nm is much smaller than those under the 300 nm and 375 nm. The photovoltage of the reference single junction under 600 nm is too small to be distinguished.

At last, we summarized the photovoltage of different structures, which is illustrated in Figure 6(a). Under the

illumination of 308 nm pulse laser, the LSMO/SNTO single junction has a photovoltage of 30 mV. By artificial design, the LSMO/insulator/SNTO multilayer structure can show a photovoltage of 290 mV (LSMO/STO/SNTO) and 410 mV (LSMO/BTO/SNTO). By further artificially designing, the photovoltage of LSMO/ITO/SNTO/LSMO/SNTO can reach as large as 600 mV, which is nearly 20 times of the single junction LSMO/SNTO.

Now, we discuss the origin of the significant enhancement of photovoltages in the artificially designed structures. When light illuminates a p - n junction, photo-generated carriers in the junction are separated by the built-in field and collected by the electrodes. This is how the photovoltage in p - n junction is generated.²¹ For the LSMO/insulator/SNTO multilayer structures, the energy band diagram is illustrated in Figures 6(b) and 6(c). The dashed lines label the depletion layers of the LSMO/SNTO single junction and the LSMO/insulator/SNTO multilayer structures. In the LSMO/insulator/SNTO multilayer structures, the inserting insulator layer is fully depleted because of the built-in field.²⁶ This means that the width of the depletion layer is expanded comparing with the single LSMO/SNTO junction, which is clearly shown in Figs. 6(b) and 6(c). Thus, the photogenerated carriers can be separated farther due to the wider depletion layer, and the recombination of the photogenerated carriers is less, which can increase the photovoltage of the LSMO/insulator/SNTO multilayer structure. As for the LSMO/SNTO/ITO/LSMO/SNTO multilayer structure, we expected the increase of the photovoltage is first due to the adding up effect from the two individual LSMO/SNTO heterojunctions connected by the ITO conducting layer. We also expected that it may be twice larger than the photovoltage of single LSMO/SNTO junction due to much thinner layer of the SNTO (10 nm) in the upper junction than that (the substrate SNTO 0.5 mm) of in the lower junction, as we already know that thinner film can even increase the photovoltage to one order larger, also, due to the reduction of the recombination of photogenerated carriers during their drifting process.²⁰ However, a 20 times larger photovoltage than that in the single junction still surprised us, and the mechanism behind this significant enhancement remains an open question, and we expect that some further studies both experimentally and theoretically can shine some light on it. As shown in Fig. 4, the thickness of ITO layer can greatly influence the photovoltage. Except

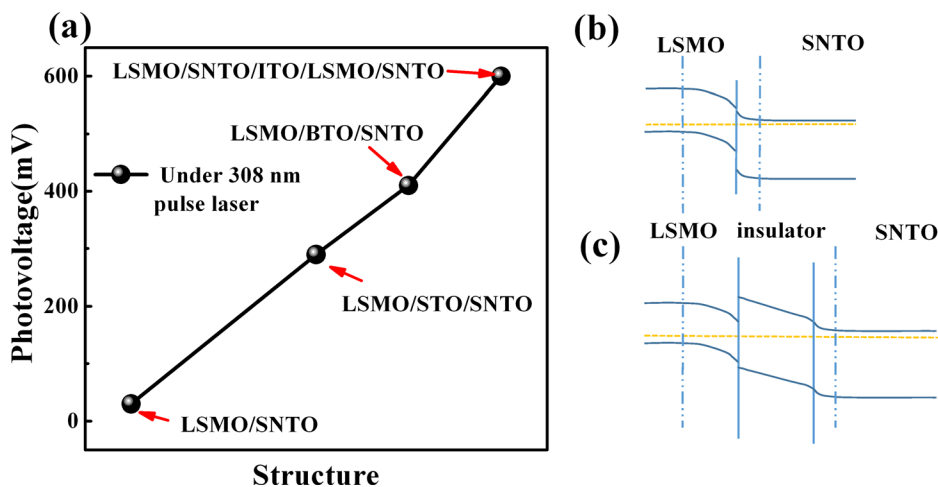


FIG. 6. (a) Photovoltage of different multilayer structures and their reference LSMO/SNTO single junction under 308 nm pulse laser. (b) Energy band diagram of LSMO/SNTO single junction. (c) Energy band diagram of LSMO/insulator/SNTO structure. The dashed lines labeled the depletion layers.

preventing the formation of the inverse junction between the LSMO layer in the lower junction and the SNT0 layer in the upper junction,²⁷ we think the interface produced by the ITO layer may also play an important role in the significant enhancement of the photovoltage.

In conclusion, we designed two multilayer structures of LSMO/insulator/SNT0 as well as LSMO/SNT0/ITO/LSMO/SNT0, and systematically investigated their photoelectricity properties. A significant enhancement of photovoltage as large as 20 times larger as that in LSMO/SNT0 single junction was obtained. Our findings demonstrate that the multilayer structures are with great potential to be used in photovoltage devices to enhance the photovoltage. For the LSMO/insulator/SNT0 multilayer structure, we suggest the expansion of the depletion layer and the reduction of the recombination of photo-generated carriers is the reason for the enhancement of the photovoltage. For the LSMO/SNT0/ITO/LSMO/SNT0 multilayer structure, we think the upper junction of LSMO/SNT0 with much thinner SNT0 layer than that (SNT0 substrate) of the lower junction dominates the great increase of the photovoltage due to much less recombination in that junction,²⁰ and the interface created by the ITO layer may also play some important roles in the photovoltaic enhancement of the LSMO/SNT0/ITO/LSMO/ITO multilayer. However, some other mechanism behind this significant enhancement remains unrevealed and further studies both experimentally and theoretically are expected.

This work was supported by the National Key Basic Research Program of China (Grant Nos. 2014CB921001 and 2013CB328706), the National Natural Science Foundation of China (Grant Nos. 10825418, 11474349, and 11134012), and the Strategic Priority Research Program (B) of the Chinese Academy of Sciences (Grant No. XDB07030200).

¹G. Herranz, M. Basletic, M. Bibes, C. Carretero, E. Tafra, E. Jacquet, K. Bouzehouane, C. Deranlot, A. Hamzic, J. M. Broto, A. Barthelemy, and A. Fert, *Phys. Rev. Lett.* **98**, 216803 (2007).

²S. Thiel, G. Hammerl, A. Schmehl, C. W. Schneider, and J. Mannhart, *Science* **313**, 1942 (2006).

³A. Ohtomo and H. Y. Hwang, *Nature* **441**, 120 (2006).

⁴K. J. Jin, H. B. Lu, K. Zhao, C. Ge, M. He, and G. Z. Yang, *Adv. Mater.* **21**, 4636 (2009).

⁵H. B. Lu, S. Y. Dai, Z. H. Chen, Y. L. Zhou, B. L. Cheng, K. J. Jin, L. F. Liu, G. Z. Yang, and X. L. Ma, *Appl. Phys. Lett.* **86**, 032502 (2005).

⁶T. Yajima, Y. Hikita, and H. Y. Hwang, *Nat. Mater.* **10**, 198 (2011).

⁷X. He, K. J. Jin, C. Ge, C. Wang, H. B. Lu, and G. Z. Yang, *Europhys. Lett.* **102**, 37007 (2013).

⁸L. Liao, K. J. Jin, C. Ge, C. L. Hu, H. B. Lu, and G. Z. Yang, *Appl. Phys. Lett.* **96**, 062116 (2010).

⁹J. Xing, E. Guo, K. J. Jin, H. B. Lu, J. Wen, and G. Z. Yang, *Opt. Lett.* **34**, 1675 (2009).

¹⁰E. Assmann, P. Blaha, R. Laskowski, K. Held, S. Okamoto, and G. Sangiovanni, *Phys. Rev. Lett.* **110**, 078701 (2013).

¹¹H. B. Lu, K. J. Jin, Y. H. Huang, M. He, K. Zhao, B. L. Cheng, Z. H. Chen, Y. L. Zhou, S. Y. Dai, and G. Z. Yang, *Appl. Phys. Lett.* **86**, 241915 (2005).

¹²L. Wang, K. J. Jin, C. Ge, C. Wang, H. Z. Guo, H. B. Lu, and G. Z. Yang, *Appl. Phys. Lett.* **102**, 252907 (2013).

¹³L. Wang, K. J. Jin, J. X. Gu, C. Ma, X. He, J. Zhang, C. Wang, Y. Feng, Q. Wan, J. A. Shi, L. Gu, M. He, H. B. Lu, and G. Z. Yang, *Sci. Rep.* **4**, 6980 (2014).

¹⁴L. Wang, K. J. Jin, J. Xing, C. Ge, H. B. Lu, W. J. Zhou, and G. Z. Yang, *Appl. Opt.* **52**, 3473 (2013).

¹⁵W. J. Zhou, K. J. Jin, H. Z. Guo, C. Ge, M. He, and H. B. Lu, *J. Appl. Phys.* **114**, 224503 (2013).

¹⁶K. J. Jin, K. Zhao, H. B. Lu, L. Liao, and G. Z. Yang, *Appl. Phys. Lett.* **91**, 081906 (2007).

¹⁷J. Xing, K. Zhao, G. Z. Liu, M. He, K. J. Jin, and H. B. Lu, *J. Phys. D: Appl. Phys.* **40**, 5892 (2007).

¹⁸N. Zhou, K. Zhao, H. Liu, H. B. Lu, M. He, S. Q. Zhou, W. X. Leng, A. J. Wang, Y. H. Huang, K. J. Jin, Y. L. Zhou, and G. Z. Yang, *J. Phys. D: Appl. Phys.* **41**, 155414 (2008).

¹⁹T. Choi, L. Jiang, S. Lee, T. Egami, and H. N. Lee, *New J. Phys.* **14**, 093056 (2012).

²⁰C. Wang, K. J. Jin, R. Q. Zhao, H. B. Lu, H. Z. Guo, C. Ge, M. He, C. Wang, and G. Z. Yang, *Appl. Phys. Lett.* **98**, 181101 (2011).

²¹S. M. Sze and K. K. Ng, *Physics of Semiconductor Devices*, 3rd ed. (Wiley, New York, 2007).

²²M. Takaki, M. Yuji, and H. Zenji, *Jpn. J. Appl. Phys.* **44**, 7367 (2005).

²³E. J. Guo, H. Z. Guo, H. B. Lu, K. J. Jin, M. He, and G. Z. Yang, *Appl. Phys. Lett.* **98**, 011905 (2011).

²⁴L. Liao, K. J. Jin, H. B. Lu, P. Han, M. He, and G. Z. Yang, *Solid State Commun.* **149**, 915 (2009).

²⁵H. Kim, C. M. Gilmore, A. Piqué, J. S. Horwitz, H. Mattoussi, H. Murata, Z. H. Kafafi, and D. B. Chrisey, *J. Appl. Phys.* **86**, 6451 (1999).

²⁶M. Sugiura, K. Uragou, M. Noda, M. Tachiki, and T. Kobayashi, *Jpn. J. Appl. Phys.* **38**, 2675 (1999).

²⁷A. Yakimov and S. R. Forrest, *Appl. Phys. Lett.* **80**, 1667 (2002).